PROCEEDINGS OF SPIE

SPIEDigitalLibrary.org/conference-proceedings-of-spie

High-performance mode-locked lasers on silicon

Liu, Songtao, Wu, Xinru, Norman, Justin, Jung, Daehwan, Dumont, Mario, et al.

Songtao Liu, Xinru Wu, Justin Norman, Daehwan Jung, Mario Dumont, Chen Shang, Yating Wan, M.J. Kennedy, Bozhang Dong, Dominik Auth, Stefan Breuer, Frédéric Grillot, Weng Chow, Arthur Gossard, John Bowers, "High-performance mode-locked lasers on silicon," Proc. SPIE 11274, Physics and Simulation of Optoelectronic Devices XXVIII, 112741K (2 March 2020); doi: 10.1117/12.2552224

SPIE.

Event: SPIE OPTO, 2020, San Francisco, California, United States

High-performance mode-locked lasers on silicon

Songtao Liu*[a], Xinru Wu[a], Justin Norman[a], Daehwan Jung[a,b], Mario Dumont[a], Chen Shang[a], Yating Wan[a], MJ Kennedy[a], Bozhang Dong[c], Dominik Auth[d], Stefan Breuer[d], Frédéric Grillot[c,e], Weng Chow[f], Arthur Gossard[a] and John Bowers[a]

[a]University of California, Santa Barbara, Santa Barbara, California 93106, USA
[b]Center for Opto-electronic Materials and Devices, KIST, Seoul 02792, South Korea
[c]LTCI, Télécom Paris, Institut Polytechnique de Paris, 19 Place Marguerite Perey, 91120 Palaiseau, France
[d]Institute of Applied Physics, Technische Universität Darmstadt, Schloßgartenstraße 7, 64289 Darmstadt, Germany
[e]Center for high Technology Materials, 1313 Goddard SE, Albuquerque, NM87106-4343, USA
[f]Sandia National Laboratories, Albuquerque, NM 87185-1086, USA
*stliu@ece.ucsb.edu

ABSTRACT

In this paper we review our recent progress on high performance mode locked InAs quantum dot lasers that are directly grown on CMOS compatible silicon substrates by solid-source molecular beam epitaxy. Different mode locking configurations are designed and fabricated. The lasers operate within the O-band wavelength range, showing pulsewidth down to 490 fs, RF linewidth down to 400 Hz, and pulse-to-pulse timing jitter down to 6 fs. When the laser is used as a comb source for wavelength division multiplexing transmission systems, 4.1 terabit per second transmission capacity was achieved. Self-mode locking is also investigated both experimentally and theoretically. The demonstrated performance makes those lasers promising light source candidates for future large-scale silicon electronic and photonic integrated circuits (EPICs) with multiple functionalities.

Keywords: Silicon photonics, photonic integrated circuits, quantum dots, semiconductor mode-locked lasers, comb generation, WDM transmission

1. INTRODUCTION

Mode locked lasers (MLLs) can emit wide coherent combs and ultra-short pulses and have long been investigated theoretically and experimentally[1-5], utilizing different material systems and configurations. Compared to bulky solid-state material based or fiber-based counterparts, semiconductor-based MLLs take advantage of small footprint, high wall-plug efficiency, low fabrication cost, mass producibility, and high integration capability, enabling widespread application capabilities. It has been demonstrated that semiconductor MLLs can be used as comb sources for wavelength division multiplexing (WDM) systems to increase the transmission capacity[6]. They can be employed as pulse sources for time division multiplexing systems as well as photonic assisted analog to digital conversion purposes[7]. In addition, these lasers can be utilized to generate stable RF signals for mm-wave and optical arbitrary waveform generation applications[8].

Quantum dot (QD), compared to conventional bulk or quantum well (QW) semiconductor material systems, show advantages in terms of mode locking dynamics due to their own unique material properties[9,10]. The inhomogeneously broadened gain would translate to a wide mode locking bandwidth (more cavity modes involved in the process); the low threshold current density, low internal loss and low confinement factor would establish low noise operation; the high temperature stability would lead to uncooled operation; the ultrafast absorption recovery response would make the laser suitable to generate sub-picosecond pulses. What is more important, the three-dimensional charge carrier confinement property would make it less sensitive to the presence of material defects, which is a huge plus in terms of the monolithic heteroepitaxy when considering the large lattice constant mismatch between the III/V material and the silicon[11]. This virtue indicates the high potential of realizing high performance active devices on CMOS compatible silicon substrate by direct epitaxy, which has long been an unsolved issue for both academia and industry due to the inherent indirect bandgap nature of Si[12]. The research on direct epitaxial growth of III-V material on Si has been carried out for several decades. However, the demonstrated devices based on bulk or QW have shown short lifetime as well as degraded

Physics and Simulation of Optoelectronic Devices XXVIII, edited by Bernd Witzigmann, Marek Osiński, Yasuhiko Arakawa, Proc. of SPIE Vol. 11274, 112741K · © 2020 SPIE
CCC code: 0277-786X/20/$21 · doi: 10.1117/12.2552224

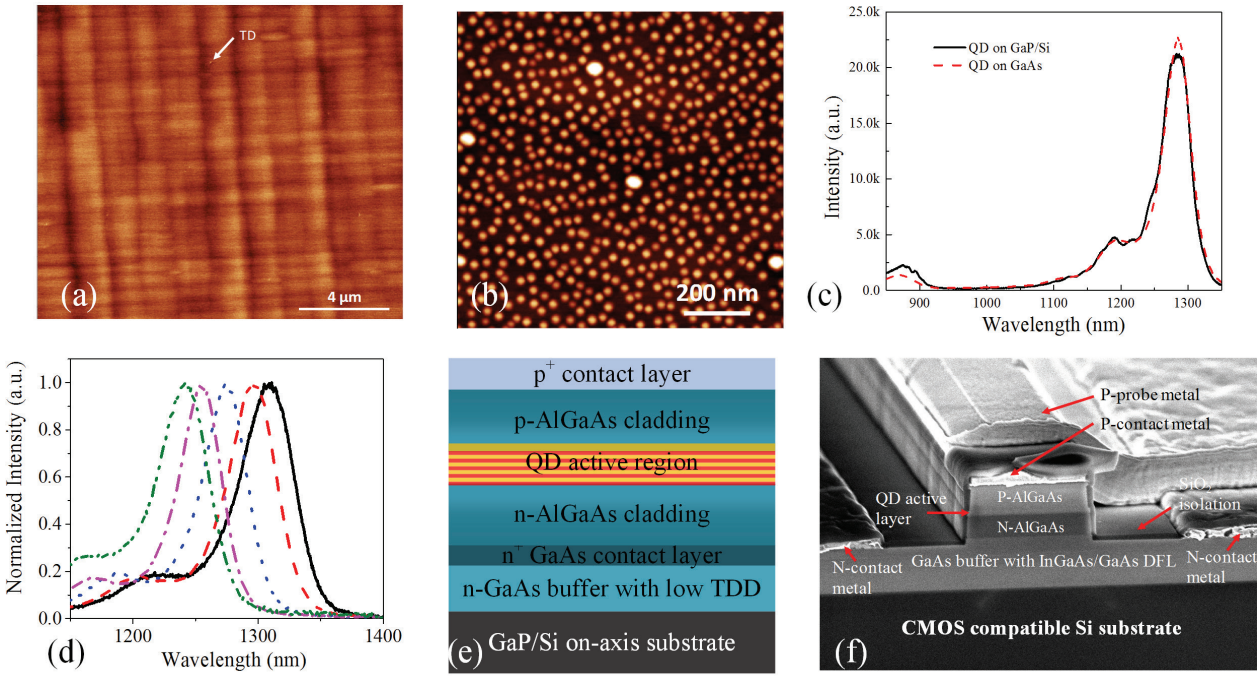

Fig. 1. (a) Electron channeling contrast image of the optimized GaAs buffer grown on GaP/Si substrate. One arrow indicates a single threading dislocation observed on the surface (b) atomic force microscopy image of an uncapped quantum dot layer, showing a dot density around 6×10^{10} cm^{-2} (c) photoluminescence intensity comparison between QD grown on native substrate and QD grown on silicon substrate (d) superimposed photoluminescence spectra of five QD growth samples demonstrating controlled adjustment of QD emission wavelength (e) typical laser structure used in this work (f) cross-sectional scanning electron microscope image of a cleaved laser facet with arrows indicating each layer.

performance compared to that of the devices on native substrate due to the large amount of dislocations with performance inadequate for practical applications[13]. The introduction of the QD gain on Si has greatly addressed this problem[11]. By carefully designing the buffer layer and growth procedures, threading dislocation (TD) density lower than ~7×10^6 cm^{-2} can be obtained[14]. Based on these platforms, various active components have been demonstrated, including high performance Fabry-Perot (FP) lasers with a lowest lasing threshold and a longest lifetime of more than a million hours[15], sub-milliamp threshold micro ring lasers[16], tunable single wavelength lasers[17], high-gain and wide amplification bandwidth semiconductor optical amplifiers[18], monolithic QD distributed feedback laser arrays[19], low dark current photodiodes[20], etc. Several detailed review papers can be found at[13,21,22].

In this paper, we report our recent efforts on the realization of high performance MLLs based on InAs QDs directly grown on Si operating at O-band. It starts with the material growth and laser fabrication, followed by several demonstrated MLL examples. We have also employed one of the MLLs as a comb source for WDM application; 4.1 Tbps transmission capacity has been shown with a four-level pulse amplitude modulation (PAM-4) format. As the demand for data transmission bandwidth keeps on growing, especially within datacenters, QD MLLs are appealing light source candidates for Si EPICs.

2. INAS QUANTUM DOT HETEROEPITAXY AND LASER FABRICATION

The MLL samples presented in this paper were all grown by solid-source molecular beam epitaxy (MBE), employing GaP/Si (001) on-axis wafers as the growth template, which is commercially available from $NASP_{III/V}$, GmbH. This wafer template is designed to be antiphase-domain (APD) free by careful surface treatments with a 45 nm pseudomorphic GaP layer grown directly on Si[14]. Combining thermal cycle annealing and dislocation filter techniques, the resulted TD density of the GaAs buffer layer can be pushed down to 7×10^6 cm^{-2}, which is confirmed by the electron channeling contrast imaging (ECCI) measurements shown in Fig. 1(a). The root-mean-square surface roughness of the buffer layers on the growth substrate was measured to be 2.9 nm in 10×10 μm^2 scans. The QD active region stacks are then deposited by the well-known Stranski-Krastanov growth method with a typical QD density of 6×10^{10} cm^{-2}. Fig. 1(b) shows an atomic force microscopy image of the uncapped InAs QDs grown on one test sample. When comparing the

room-temperature photoluminescence (PL) intensity between the QDs on Si and QDs on native substrate depicted in Fig. 1(c), little difference can be found between both curves, which suggests high QD material growth quality on Si. Typical PL full-width at half maximum (FWHM) is around 30 meV.

For MLLs, we also introduced a chirped QD layer design to broaden the PL FWHM[23]. By varying the thickness of the InGaAs QW layers in the five-layer active region structure from 3 to 7 nm, the PL peak position of each layer can be shifted in sequence, as shown in Fig. 1(d) leading to a 77% increase of the FWHM to 53 meV, which could provide more modes in the mode locking process. A typical laser structure is shown in Fig. 1(e). On top of the buffer layer, *n*- and *p*-contact and cladding layer were grown in sequence, sandwiching the QD active region. After the growth, the whole wafer was processed leveraging standard semiconductor fabrication technology. A deeply etched waveguide profile is adopted to facilitate the coplanar *n*- and *p*-probe metallization. Coplanar ground-signal (GS) pads were also designed to facilitate the extraction of the generated RF signal directly by a high-speed RF probe. Electrical isolation between the gain and the saturable absorption (SA) section is formed by a second dry etch with an etch depth of 600-nm deep into the *p*-cladding layer. The isolation resistance is measured to be > 15 kΩ. Fig. 1(f) shows a cross section SEM image of the fabricated laser with each layer indicated. After the fabrication process, the Si substrate was thinned down to 200 μm to facilitate laser bar cleaving. The laser facets were left as cleaved.

3. 9 GHZ MODE LOCKED LASERS WITH 400 HZ RF LINEWIDTH

The first example is a 9 GHz mode locked laser. A classical two-section FP cavity design is adopted. By adjusting the cavity length, one can precisely control the repetition rate. In this case, the total length of the laser was designed to be 4500 μm as the group effective index was assumed 3.66 for a 3 μm wide ridge width. Different SA section lengths ranging from 3% to 23% were incorporated to investigate the dynamics between the gain and the absorption. Fig. 2(a) shows a photograph of the cleaved device bar with each section labelled. The performance of these MLLs is discussed in detail in[24,25]. Typically, they have a threshold range from 65 mA to 85mA as the SA section length increases. The SA section was left floating. By tuning the gain section current and SA reverse voltage, passive mode locking (PML) regimes were investigated for those lasers. With the exception of the device with SA length ratio of 3% demonstrating no mode locking behavior, all the rest of the lasers show wide PML regimes. By comparing the narrowest pulse obtained from each QD MLL device, one can find that a longer SA section can provide shorter pulses as shown in Fig. 2(b). A pulsewidth reduction of 48% of the narrowest achievable pulse from each QD MLL can be obtained from 2.5 ps down to

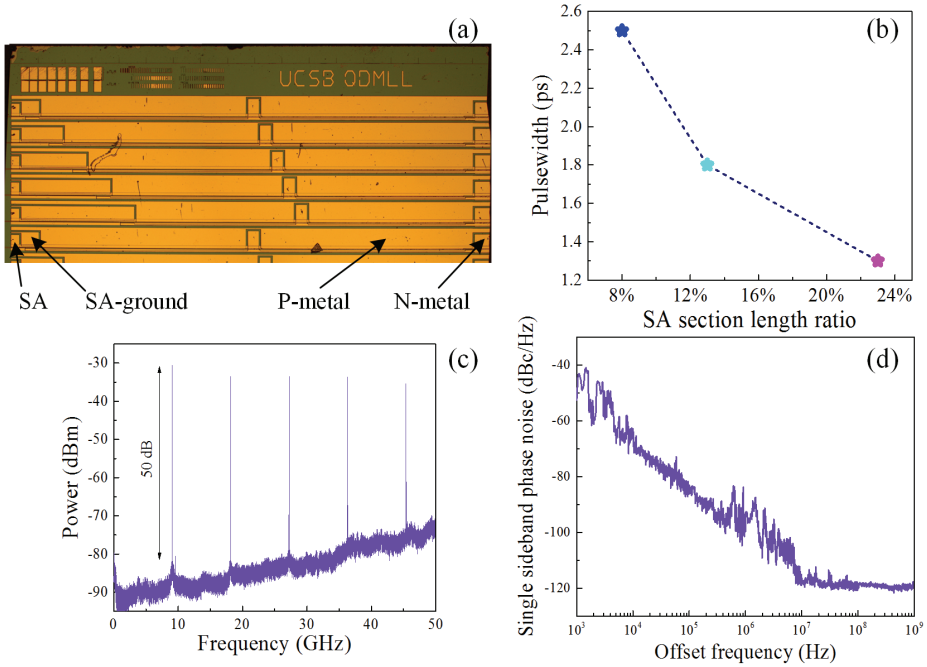

FIG. 2. (a) Photograph of the fabricated 9 GHz MLL array with different SA section length (b) minimum achievable pulsewidth as a function of the SA length ratio (c) RF spectra of the device, showing a > 50 dB SNR ratio with higher order harmonics (d) SSB phase noise, indicating a 400 Hz RF linewidth.

1.3 ps when the SA section length ratio increases from 8% to 23%. Typical spectrum 3 dB bandwidth is around 3.6 nm.

RF performance is shown in Fig. 2(c). Sharp RF peaks at the fundamental frequency of 9.1 GHz and its higher order harmonics can be clearly seen. The SNR ratio of the fundamental frequency larger than 50 dB indicates the QD MLL is under stable passive mode locking operation. Narrowest RF linewidth is found in a device with SA section length of 18%. A 400 Hz RF linewidth is deduced from the single sideband (SSB) phase noise as shown in Fig. 2(d)[26], which is the narrowest value ever reported from a passively mode locked semiconductor laser without any stabilizing technique. It indicates again the benefit of using the QD material to realize the low noise devices.

4. 20 GHZ MODE LOCKED LASERS WITH TERABIT TRANSMISSION CAPACITY

By changing the cavity length to 2048 μm, 20 GHz channel spacing MLLs can be easily demonstrated[27]. In this work, unlike the previous 9 GHz case, we replaced the normal un-chirped gain-section region design to the chirped dot design to further enhance the mode locking spectral bandwidth of the MLL. The SA section length in this work was chosen to be 14% of the total cavity length. Typical laser threshold is around 40 mA with a stage temperature of 18 °C. A wide PML regime was demonstrated with a gain section current ranging from 75 mA to 200 mA and SA reverse voltage ranging from 1 V to 5 V. The minimum pulse width is 5 ps with the fundamental RF SNR value larger than 60 dB. The corresponding SSB phase noise of this PML state shows an integrated timing jitter of 286 fs from 100 kHz to 100 MHz, and 82.7 fs from 4 to 80 MHz of the ITU-T specified range, which is the lowest timing jitter ever reported to date for any passively mode-locked semiconductor laser diodes. The pulse-to-pulse timing jitter of this state is 6 fs calculated by the formula in[28], which is also the lowest value reported so far.

Benefiting from the wide gain bandwidth, the mode locking spectrum shows a 3 dB bandwidth of 6.1 nm (58 lines, 80 lines within 10 dB), which is a 70% increase compared to that of the case with un-chirped gain section design. Fig. 3(a) shows the whole spectrum within 10 dB, splitting into 16 parts indicated by different colors. The corresponding RF spectrum of each spectral part is depicted in Fig. 3(b), which shows exactly the same beat frequency at 20.056 GHz ± 1

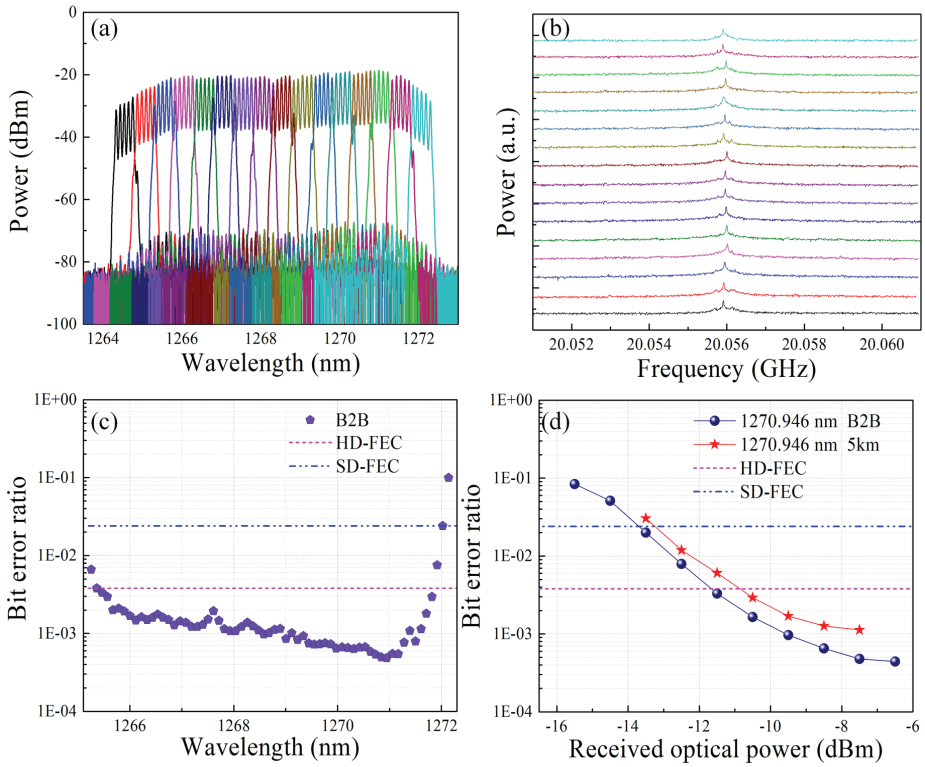

FIG. 3. (a) Optical spectrum within 10 dB bandwidth, superimposed by 16 splits (b) corresponding RF spectra of the 16 splits, indicating strong coherence within the mode locking bandwidth (c) back-to-back BER performance of the PAM-4 signal with different comb lines (d) BER versus received optical power for B2B and after 5 km SSMF transmission of the comb line located at 1270.946 nm.

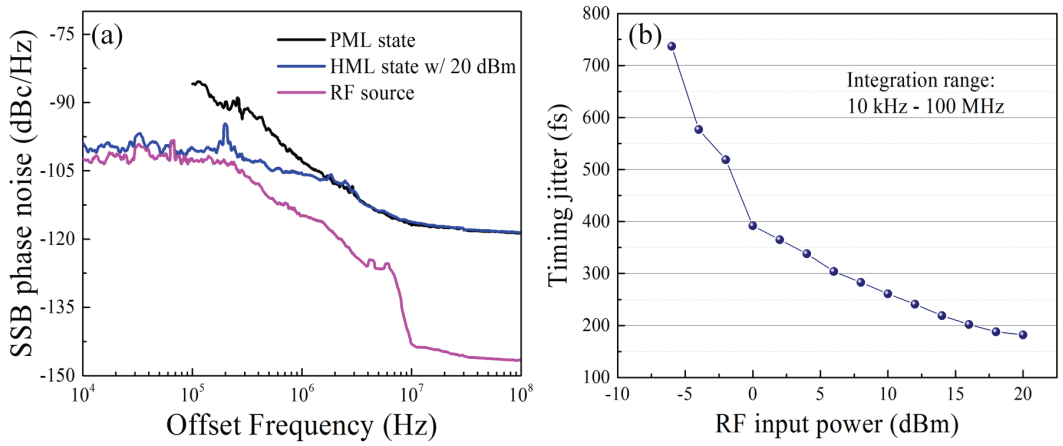

FIG. 4. (a) SSB phase noise of the MLL under PML and HML states as well as that of the RF signal generator (b) calculated timing jitter of the MLL under differ RF input power under HML state.

MHz, indicating the strong coherence within the whole spectrum. By employing the MLL into a PAM-4 system level transmission link, we have demonstrated 64 channels with bit error ratios (BERs) below the soft-decision FEC threshold (20% overhead), leading to an aggregate data transmission rate of 4.1 terabit per second. Fig. 3(c) shows the back-to-back (B2B) BER performance of each channel. The BER versus received power for the carriers located at 1270.946 nm for B2B and after 5 km SSMF transmission is presented in Fig. 3(d). The power penalty is about 1 dB. This means the MLL could fulfill the ITU-T dense WDM grid requirement strictly, which has the potential to replace tens or hundreds of the single wavelength lasers. It will greatly simplify the transmitter design in the system link as well as lower the total cost.

In terms of further improving the MLL's noise performance, two simple methods could be utilized. The most convenient way is by the hybrid mode locking (HML) configuration[26,29], where an RF signal corresponding to the fundament frequency is applied to the SA section, functioning as a timing shutter to stabilize the MLL. Fig. 4(a) shows the SSB phase noise plots of the PML state, HML state with RF input power of 20 dBm, and the RF signal source. One can observe that the low frequency noise of the MLL has been greatly suppressed, which leading to a reduced timing jitter of 182 fs when integrated from 10 kHz – 100 MHz (RF source timing jitter is 57 fs in the same range). Fig. 4(b) shows the timing jitter of the MLL under different RF input power. It can be seen that less than -6 dBm RF input power would be required to make the timing jitter less than 1 ps, which is a reasonable figure of merit for practical system applications[30]. The other way is to employ the optical self-feedback configuration, where a portion of the output signal is fed back into the cavity using a fiber loop[31,32]. In the resonant optical feedback condition, the RF linewidth from one of the 20 GHz MLLs was reduced down to about 800 kHz against 2.7 MHz at the free-running state, which shows a 3x improvement[33].

5. SELF MODE LOCKING WITH SINGLE SECTION STRUCTURE

In the future low power consumption WDM transmission networks, high wall plug efficiency (WPE) and high power per comb line sources are strongly needed. Currently, the typical two section mode locked lasers generally have low WPEs in the range of 2% to 5%, which are far less than that of the reported FP lasers[15], which are largely the result of the absorption loss introduced by the SA section. If mode locking can be realized without the SA section, it would be even more appealing to the low energy consumption applications. Since the first report on self-mode locking in 1.5-μm QW FP lasers[34,35], several groups have observed this unique behavior in different material systems, including 1.55-μm InAs/InP quantum dash FP lasers[36,37], 1.3-μm InAs/GaAs edge emitting QD based laser[38,39], etc. In our initial experimental exploration, we have also observed this behavior in a single gain section QD laser grown by MBE on Si. It operates in the O-band, demonstrating a 31 GHz repetition rate with a 100 kHz RF linewidth, meanwhile delivering a 490 fs pulsewidth[40]. Higher rate pulse trains could be anticipated with a shorter cavity length. The high four-wave-mixing efficiency that is exhibited in zero-dimensional QD material is assumed to be the main underlying mechanism. We have developed a theory to explore this phenomenon, which is based on a multimode semiclassical laser theory that accounts for fast carrier collisions within an inhomogeneous distribution of quantum dots. Numerical simulations are presented to illustrate active medium nonlinearities resulting in mode competition, gain saturation, four-wave mixing,

carrier-induced refractive index and creation of combination tones that may lead to locking of beat frequencies among lasing modes[41].

6. CONCLUSIONS

In summary, we have reviewed recent progress on monolithic InAs/GaAs QD MLLs directly grown on CMOS compatible silicon substrates as well as their potential application in WDM systems. A range of channel spacing can be realized by changing the total cavity length or employing higher order harmonic configurations[42]. Mode locking bandwidth enhancement could be obtained by engineering the QD active region. Noise performance improvement could be achieved by simple HML or self-feedback configurations. Driven by the strong need for low power consumption in system designs, clearly more work needs to be explored. One direction is to continue optimizing the laser design, where the series resistance, internal loss, thermal impedance, and injection efficiency could be improved, as each is currently below state-of-the-art in these devices. The other is to seek the underlying mechanism of self-mode locking, where the power load on the SA could be eliminated, leading to better energy efficiency. As the III-V/Si epitaxy have improved significantly with high yield and high reliability, the demonstrated MLL sources would make the fast growing silicon EPICs more appealing to various applications.

This research was funded by the Advanced Research Projects Agency-Energy (ARPA-E), U.S. Department of Energy, under Award No. DE-AR0000843. The views and opinions of the authors expressed herein do not necessarily state or reflect those of the United States Government or any agency thereof.

REFERENCES

[1] Haus, H. A., "Mode-locking of lasers," IEEE J. Sel. Top. Quantum Electron. **6**(6), 1173–1185 (2000).
[2] Bowers, J. E., Morton, P. A., Mar, A. and Corzine, S. W., "Actively mode-locked semiconductor lasers," IEEE J. Quantum Electron. **25**(6), 1426–1439 (1989).
[3] Williams, K. A., Thompson, M. G. and White, I. H., "Long-wavelength monolithic mode-locked diode lasers," New J. Phys. **6**, 1–30 (2004).
[4] E.A. Avrutin, J.H. Marsh, E. L. P., "Monolithic and multi-gigahertz mode-locked semiconductor lasers: constructions, experiments, models and applications," IEEE Proc. - Optoelectron. **147**(4), 251–278 (2000).
[5] Liu, S., Wang, H., Sun, M., Zhang, L., Chen, W., Lu, D., Zhao, L., Broeke, R., Wang, W. and Ji, C., "AWG-Based Monolithic 4×12 GHz Multichannel Harmonically Mode-Locked Laser," IEEE Photonics Technol. Lett. **28**(3), 241–244 (2016).
[6] Marin-Palomo, P., Kemal, J. N., Trocha, P., Wolf, S., Merghem, K., Lelarge, F., Ramdane, A., Freude, W., Randel, S. and Koos, C., "Comb-based WDM transmission at 10 Tbit/s using a DC-driven quantum-dash mode-locked laser diode," Opt. Express **27**(22), 31110–31129 (2019).
[7] Quinlan, F., Ozharar, S., Gee, S. and Delfyett, P. J., "Harmonically mode-locked semiconductor-based lasers as high repetition rate ultralow noise pulse train and optical frequency comb sources," J. Opt. A Pure Appl. Opt. **11**(10) (2009).
[8] Haji, M., Hou, L., Kelly, A. E., Akbar, J., Marsh, J. H., Arnold, J. M. and Ironside, C. N., "High frequency optoelectronic oscillators based on the optical feedback of semiconductor mode-locked laser diodes," Opt. Express **20**(3), 3268–3274 (2012).
[9] Rafailov, E. U., Cataluna, M. A. and Sibbett, W., "Mode-locked quantum-dot lasers," Nat. Photonics **1**, 395 (2007).
[10] Thompson, M. G., Rae, A. R., Xia, M., Penty, R. V and White, I. H., "InGaAs Quantum-Dot Mode-Locked Laser Diodes," IEEE J. Sel. Top. Quantum Electron. **15**(3), 661–672 (2009).
[11] Liu, A. Y., Srinivasan, S., Norman, J., Gossard, A. C. and Bowers, J. E., "Quantum dot lasers for silicon photonics [Invited]," Photonics Res. **3**(5), B1 (2015).
[12] Liang, D. and Bowers, J. E., "Recent progress in lasers on silicon," Nat. Photonics **4**, 511 (2010).
[13] Norman, J. C., Jung, D., Wan, Y. and Bowers, J. E., "Perspective: The future of quantum dot photonic integrated circuits," APL Photonics **3**(3), 030901 (2018).
[14] Jung, D., Callahan, P. G., Shin, B., Mukherjee, K., Gossard, A. C. and Bowers, J. E., "Low threading dislocation density GaAs growth on on-axis GaP/Si (001)," J. Appl. Phys. **122**(22), 225703 (2017).
[15] Jung, D., Zhang, Z., Norman, J., Herrick, R., Kennedy, M. J., Patel, P., Turnlund, K., Jan, C., Wan, Y., Gossard,

A. C. and Bowers, J. E., "Highly Reliable Low-Threshold InAs Quantum Dot Lasers on On-Axis (001) Si with 87% Injection Efficiency," ACS Photonics **5**(3), 1094–1100 (2018).
[16] Wan, Y., Norman, J., Li, Q., Kennedy, M. J., Liang, D., Zhang, C., Huang, D., Zhang, Z., Liu, A. Y., Torres, A., Jung, D., Gossard, A. C., Hu, E. L., Lau, K. M. and Bowers, J. E., "13 μm submilliamp threshold quantum dot micro-lasers on Si," Optica **4**(8), 940 (2017).
[17] Wan, Y., Zhang, S., Norman, J. C., Kennedy, M. J., He, W., Liu, S., Xiang, C., Shang, C., He, J.-J., Gossard, A. C. and Bowers, J. E., "Tunable quantum dot lasers grown directly on silicon," Optica **6**(11), 1394 (2019).
[18] Liu, S., Norman, J., Dumont, M., Jung, D., Torres, A., Gossard, A. C. and Bowers, J. E., "High-Performance O-Band Quantum-Dot Semiconductor Optical Amplifiers Directly Grown on a CMOS Compatible Silicon Substrate," ACS Photonics **6**(10), 2523–2529 (2019).
[19] Wang, Y., Chen, S., Yu, Y., Zhou, L., Liu, L., Yang, C., Liao, M., Tang, M., Liu, Z., Wu, J., Li, W., Ross, I., Seeds, A. J., Liu, H. and Yu, S., "Monolithic quantum-dot distributed feedback laser array on silicon," Optica **5**(5), 528–533 (2018).
[20] Sun, K., Jung, D., Shang, C., Liu, A., Morgan, J., Zang, J., Li, Q., Klamkin, J., Bowers, J. E. and Beling, A., "Low dark current III-V on silicon photodiodes by heteroepitaxy," Opt. Express **26**(10), 13605–13613 (2018).
[21] Norman, J. C., Jung, D., Zhang, Z., Wan, Y., Liu, S., Shang, C., Herrick, R., Chow, W. W., Gossard, A. and Bowers, J., "A Review of High Performance Quantum Dot Lasers on Silicon," IEEE J. Quantum Electron. **55**(2), 1–11 (2019).
[22] Liao, M., Chen, S., Huo, S., Chen, S., Wu, J., Tang, M., Kennedy, K., Li, W., Kumar, S., Martin, M., Baron, T., Jin, C., Ross, I., Seeds, A. and Liu, H., "Monolithically Integrated Electrically Pumped Continuous-Wave III-V Quantum Dot Light Sources on Silicon," IEEE J. Sel. Top. Quantum Electron. **23**(6), 1–10 (2017).
[23] Liu, S., Wu, X., Jung, D., Norman, J. C., Kennedy, M. J., Tsang, H. K., Gossard, A. C. and Bowers, J. E., "High-channel-count 20 GHz passively mode-locked quantum dot laser directly grown on Si with 4.1 Tbit/s transmission capacity," Optica **6**(2), 128–134 (2019).
[24] Liu, S., Norman, J. C., Jung, D., Kennedy, M. J., Gossard, A. C. and Bowers, J. E., "Monolithic 9 GHz passively mode locked quantum dot lasers directly grown on on-axis (001) Si," Appl. Phys. Lett. (2018).
[25] Auth, D., Liu, S., Norman, J., Edward Bowers, J. and Breuer, S., "Passively mode-locked semiconductor quantum dot on silicon laser with 400 Hz RF line width," Opt. Express **27**(19), 27256–27266 (2019).
[26] Drzewietzki, L., Breuer, S. and Elsässer, W., "Timing jitter reduction of passively mode-locked semiconductor lasers by self- and external-injection: numerical description and experiments.," Opt. Express **21**(13), 16142–16161 (2013).
[27] Liu, S., Wu, X., Jung, D., Norman, J. C., Kennedy, M. J., Tsang, H. K., Gossard, A. C. and Bowers, J. E., "High-channel-count 20 GHz passively mode-locked quantum dot laser directly grown on Si with 4.1 Tbit/s transmission capacity," Optica **6**(2), 128–134 (2019).
[28] Kéfélian, F., O'Donoghue, S., Todaro, M. T., McInerney, J. G. and Huyet, G., "RF linewidth in monolithic passively mode-locked semiconductor laser," IEEE Photonics Technol. Lett. **20**(16), 1405–1407 (2008).
[29] Liu, S., Lu, D., Zhang, R., Zhao, L., Wang, W., Broeke, R. and Ji, C., "Synchronized 4 × 12 GHz hybrid harmonically mode-locked semiconductor laser based on AWG," Opt. Express **24**(9), 9734 (2016).
[30] Srinivasan, S., Davenport, M., Heck, M. J. R., Hutchinson, J., Norberg, E., Fish, G. and Bowers, J., "Low phase noise hybrid silicon mode-locked lasers," Front. Optoelectron. **7**(3), 265–276 (2014).
[31] Lin, C. Y., Grillot, F., Li, Y., Raghunathan, R. and Lester, L. F., "Microwave characterization and stabilization of timing jitter in a quantum-dot passively mode-locked laser via external optical feedback," IEEE J. Sel. Top. Quantum Electron. 17(5), 1311–1317 (2011).
[32] Stutz, S., Auth, D., Weber, C., Drzewietzki, L., Nikiforov, O., Rosales, R., Walther, T., Lester, L.F. and Breuer, S., "Dynamic intermode beat frequency control of an optical frequency comb single section quantum dot laser by dual-cavity optical self-injection," IEEE Photonics Journal 11, 1-8 (2019)
[33] Dong B., Labriolle X., Huang H., Duan J., Liu S., Norman J., Bowers, J. and Grillot F., "Resonant optical feedback in 1.3-μm passively mode-locked quantum dot lasers epitaxially grown on silicon," Photonics North, 2020, submitted.
[34] Nomura, Y., Ochi, S., Tomita, N., Akiyama, K., Isu, T., Takiguchi, T. and Higuchi, H., "Mode locking in Fabry-Perot semiconductor lasers," Phys. Rev. A **65**(4), 43807 (2002).
[35] Sato, K., "Optical Pulse Generation Using Fabry–Pérot Lasers Under Continuous-Wave Operation," IEEE J. Sel. Top. Quantum Electron. **9**(5) (2003).
[36] Merghem, K., Akrout, A., Martinez, A., Aubin, G., Ramdane, A., Lelarge, F. and Duan, G. H., "Pulse generation

at 346 GHz using a passively mode locked quantum-dash-based laser at 1.55 μm," Appl. Phys. Lett. **94**(2), 1–4 (2009).
[37] Lu, Z., Liu, J., Raymond, S., Poole, P., Barrios, P. and Poitras, D., "312-fs pulse generation from a passive C-band InAs/InP quantum dot mode-locked laser," Opt. Express **16**(14), 10835–10840 (2008).
[38] Rosales, R., Merghem, K., Calo, C., Bouwmans, G., Krestnikov, I. and Martinez, A., "Optical pulse generation in single section InAs / GaAs quantum dot edge emitting lasers under continuous wave operation," 48–51 (2012).
[39] Weber, C., Columbo, L.L., Gioannini, M., Breuer, S. and Bardella, P., "Threshold behavior of optical frequency comb self-generation in an InAs/InGaAs quantum dot laser," Opt. Lett. 44, 3478-3481(2019).
[40] Liu, S., Jung, D., Norman, J. C., Kennedy, M. J., Gossard, A. C. and Bowers, J. E., "490 fs pulse generation from passively mode-locked single section quantum dot laser directly grown on on-axis GaP/Si," Electron. Lett. **54**(7), 432–433 (2018).
[41] Chow W., Liu S., Zhang Z., Bowers J. and Sargent M., "Multimode description of self-mode-locking in a single-section quantum-dot laser," submitted to Optics Express, under review.
[42] Liu, S., Wu, X., Norman, J., Jung, D., Kennedy, M. J., Tsang, H. K., Gossard, A. C. and Bowers, J. E., "100 GHz colliding pulse mode locked quantum dot lasers directly grown on Si for WDM application," 2019 Conf. Lasers Electro-Optics, CLEO 2019 - Proc. (2019).